Published in final edited form as:
Biochemistry. 2013 March 19; 52(11): 1939–1949. doi:10.1021/bi400126w.

Biosynthetic assembly of the *Bacteroides fragilis* Capsular Polysaccharide A precursor bactoprenyl diphosphate-linked acetamido-4-amino-6-deoxy-galactopyranose

Anahita Z. Mostafavi and **Jerry M. Troutman***
University of North Carolina at Charlotte, Department of Chemistry, 9201 University City Blvd, Charlotte, NC 28223-0001

Abstract

The sugar capsule Capsular Polysaccharide A (CPSA), which coats the surface of the mammalian symbiont *Bacteroides fragilis*, is a key mediator of mammalian immune system development. In addition, this sugar polymer has shown therapeutic potential in animal models of Multiple Sclerosis and other autoimmune disorders. The structure of the CPSA polymer includes a rare stereoconfiguration sugar acetamido-4-amino-6-deoxy-galactopyranose (AADGal) that we propose is the first sugar linked to a bactoprenyl diphosphate scaffold in the production of CPSA. In this report we have utilized a heterologous system to reconstitute bactoprenyl-diphosphate-linked AADGal production. Construction of this system included a previously reported *Campylobacter jejuni* dehydratase, PglF, coupled to a *B. fragilis* encoded aminotransferase (WcfR) and initiating hexose-1-phosphate transferase (WcfS). Function of the aminotransferase was confirmed by capillary electrophoresis and a novel high performance liquid chromatography (HPLC) method. Production of the rare uridine diphosphate (UDP)-AADGal was confirmed through a series of 1D and 2D nuclear magnetic resonance experiments and high resolution mass spectrometry (HR-MS). A spectroscopically unique analogue of bactoprenyl phosphate was utilized to characterize the transfer reaction catalyzed by WcfS, and allowed HPLC based isolation of the isoprenoid-linked sugar product. Importantly, the entire heterologous system was utilized in a single pot reaction to biosynthesize the bactoprenyl-linked sugar. This work provides the first critical step in the *in vitro* reconstitution of CPSA biosynthesis.

Keywords

Caspsular Polysaccharide A; Bacteroides fragilis; Biosynthesis pathway; aminotransferase; WcfR; initiating hexose-1-phosphate transferase; WcfS; bactoprenyl diphosphate; undecaprenyl diphosphate; bactoprenol analogues; acetamido-4-amino-6-deoxy-galactopyranose

The gut microbiota plays a central role in human health and a strong association has been noted between altered bacterial populations and disease (1–3). Interestingly, sequenced

*Corresponding Author: Jerry M. Troutman, Department of Chemistry University of North Carolina at Charlotte, 9201 University City Blvd. Charlotte, NC 28223. Jerry.Troutman@uncc.edu Tel: 704-687-4494 Fax: 704-687-0960.

Author Contributions

The manuscript was written through contributions of all authors. All authors have given approval to the final version of the manuscript.

Supporting Information. Supporting information includes primers sequences used for cloning, NMR chemical shift comparisons with previously characterized sugars, Western blot and Ponceau analysis of expressed WcfR and WcfS, Dynamic Light Scattering analysis, SDS-PAGE gel showing WcfR crosslinking, full COSY and T-ROESY spectra on UDP-AADGal, transmembrane domain prediction for WcfS, HR-MS of UDP-AADGal, and NA-B(*cis-6*)-PP-AADGal. This material is available free of charge via the Internet at http://pubs.acs.org.

genomes of the human microbiome are significantly enriched in metabolic enzymes involved in the metabolism of host or host diet glycans (4). The host of these populations benefit through extraction of nutrients from the end products of bacterial fermentation (2, 4). The symbiont *Bacteroides fragilis* reflects this commensal relationship between host and microbe in the relatively large number of genes involved in polysaccharide metabolism (4). The polysaccharides produced on the surface of *B. fragilis*, in particular, the capsule Capsular Polysaccharide A (CPSA) shown in Figure 1, has been shown to be a molecular link in the activation of $CD4^+$ T cell expression, and the early development of gut associated lymophoid tissue (5–8). Surprisingly this polysaccharide has also been shown to have protective effects on autoimmune disorder models such as antibiotic induced experimental encephalomyelitis, which is a key animal model for Multiple Sclerosis (5).

The role of CPSA in human health and the potential therapeutic value of this polymer has prompted interest in its preparation as a therapeutic. Fascinating chemical synthetic work has been devoted to produce CPSA, and synthesis of the tetrasaccharide repeating unit was achieved in a more than 20 step procedure in which the four sugars making up the unit were chemically synthesized then linked (9, 10). However, it has been shown that at least 7–8 repeat units covalently-linked are required for some of the protective effects associated with CPSA (11). Alternatively, and more typically, CPSA has been isolated from the surface of large cultures of *B. fragilis* through a multi-step isolation procedure, as eight different polysaccharides can be produced on the surface of *B. fragilis* at any time during its life cycle (8, 12). Unfortunately, bacteria may not produce consistent levels of polysaccharide materials on their surface with the exact composition from one preparation to another. All together an alternative route to producing pure consistent CPSA would be of great significance to the medical community.

In this report we have taken a biosynthetic approach to the production of the first sugar precursor in the assembly of CPSA. The gene locus responsible for polymer production by *B. fragilis* has been elucidated (13). The function of each gene in this locus has been proposed according to similarity of translated gene sequences to known proteins and similar biosynthetic systems (13–17). The identity of the genes present in this locus suggests that the most likely route for assembling the complex bacterial polysaccharide is a Wzy dependent pathway in which repeat unit oligosaccharides are assembled one sugar at a time on the cytosolic face of the bacterial inner membrane (18–22). The assembly of these oligosaccharides is thought to take place on the C55 isoprenoid bactoprenol, which acts as a hydrophobic scaffold anchoring the polymer to the membrane. It is expected that the first sugar-linked to bactoprenyl phosphate as shown in Scheme 1, is acetamido-4-amino-6-deoxy-galactopyranose (AADGal) (12). Based on homologous systems in other organisms a dehydratase, an aminotransferase, and an initiating hexose-1-phosphate transferase are necessary to manufacture this 4-amino-sugar and link it to the bactoprenyl scaffold (12, 15, 17). Within the *B. fragilis* genome CPSA biosynthesis locus, there is a predicted aminotransferase gene, *wcfR*, and initiating hexose-1-phosphate transferase gene, *wcfS*, but no dehydratase (13). However, a gene encoding a potential dehydratase has been identified elsewhere in the *B. fragilis* genome, and other organisms produce similar genes that could be used for *in vitro* biosynthesis of the oligosaccharide (12, 15, 17).

While the genes required for CPSA biosynthesis have been suggested, there is no biochemical evidence identifying what genes are responsible for each step of production. There are also no closely related homologues (>60% similarity) of the predicted aminotransferase, WcfR, or predicted initiating hexose-1-phsophate transferase, WcfS, that have been isolated and characterized biochemically. Importantly, it has been noted that functional assignment of genes based on homology alone has been considerably problematic

in numerous systems (23, 24). In this report we have isolated, expressed and biochemically characterized the proteins associated with the first steps in CPSA biosynthesis.

Materials and Methods

General

UDP-[^{3}H]GlcNAc was purchased from American Radiolabeled Chemicals. Uridine containing species were quantified by UV absorbance on a Spectramax M5 cuvette and plate reader at 260 nm using an extinction coefficient of 10,000 M^{-1} cm^{-1}. *p-nitro-aniline* containing species were quantified at 395 nm using an extinction coefficient of 9500 M^{-1} cm^{-1}. All general reagents and solvents were purchased from Sigma-Aldrich, VWR or Fisher unless stated otherwise. Custom desalted primers were purchased from Invitrogen. Sequencing was performed by the Massachusetts Institute of Technology (MIT) Sequencing Facility. All vectors were purchased from Novagen. All High Performance Liquid Chromatography (HPLC) was performed on an Agilent 1100 system equipped with a diode array detector and Gilson fraction collector. Capillary Electrophoresis (CE) was performed on a Beckman-Coulter P/ACE equipped with a diode array detector, and data was collected using 32 Karat software. Thin layer chromatography (TLC) was performed on K6f non-fluorescent plates (Whatman) and plate radiolabel detection was performed on a Bioscan AR-2000 imaging scanner. Nuclear Magnetic Resonance (NMR) Spectroscopy was performed on a 500 MHz Jeol for ^{1}H-NMR and 2D-NMR, and a 300 MHz spectrometer for ^{31}P-NMR. Low resolution electrospray ionization mass spectrometry (ESI-MS) analysis was performed in negative ion mode on a Thermo Electron Finnigan LTQ ESI-MS with injection volumes of 200 μL and concentrations ranging from 50–300 μM. High Resolution Mass Spectrometry (HR-MS) was performed at the David H. Murdock Research Institute (DHMRI) Metabolomics Laboratory by direct injection coupled to quadrapole time-of-flight MS operating in the negative mode. Isoprenoid was supplied to the DHMRI dissolved in 20% *n*-propanol in 25 mM ammonium bicarbonate buffer at 0.1 g/L, and UDP-AADGal was supplied at a similar concentration in 25 mM ammonium bicarbonate buffer.

Cloning

Polymerase Chain Reaction (PCR) amplifications of *wcfR* and *wcfS* genes were performed using *B. fragilis* Genomic DNA (ATCC 25285) and oligonucleotide primers specific to each gene (Supporting Table 1), according to manufacturer's instructions (Promega GoTaq PCR core system 1 Kit). PCR amplifications were isolated (Promega wizard® SV Gel and PCR Clean-Up System) then digested with restriction enzymes as indicated below at 37° C for four hours. Insert and specified vector digests were separated by gel electrophoresis on a 1% agarose gel. The digested inserts and plasmids were extracted (Qiagen QIAquick gel extraction kit) from the gel, and inserts were ligated into corresponding plasmids overnight at 4° C (Promega T4 DNA ligase kit). Ligated plasmids were transformed into chemically competent DH5α *Escherichia coli* cells and were plated on Luria-Bertani (LB) agar-kanamycin plates. Plasmids were isolated using Fermentas GeneJET™ Plasmid Miniprep Kit and sequenced.

wcfR gene was amplified with a 5'-BamHI site and 3'-XhoI site and inserted into a pET-24a vector encoding an N-terminal T7-tag and C-terminal hexahistidine tag.

wcfS gene was amplified with a 5'-NdeI site and 3'-XhoI site and inserted into a pET-24a vector encoding a C-terminal hexahistidine tag.

WcfS and WcfR expression by auto-induction

Plasmids encoding WcfS and WcfR were transformed into chemically competent BL-21 (DE3) RIL (Agilent) *E. coli* cells, and expressed using auto-induction as described by Studier (25) with slight modification. Overnight starter cultures were prepared with frozen protein expressing glycerol stocks of cells, and 3 mL were used to inoculate 1 L of LB broth containing kanamycin, 400 mg Glucose, 1 g lactose, 4 mL M buffer (0.625 M Na_2HPO_4, 0.625 M KH_2PO_4, 1.25 M NH_4Cl, 0.125 M Na_2SO_4), and 2 mL 1 M $MgSO_4$. The WcfR/WcfS expressing cells were incubated at 37° C until an optical density between 0.6–0.8 was reached and the temperature was reduced to 16° C.

Purification of WcfR

After overnight incubation, WcfR expressing cells were harvested by centrifugation at 5,000 × g at 4°C for 30 minutes. The cell pellets were resuspended in 30 mL of lysis buffer (50 mM Tris-HCl (pH 8), 200 mM NaCl) and lysed on ice via sonication (Fisher Scientific Sonic Dismembranator Model 500) at 25% power for 2 minutes with a pulse of 1 second on and 1 second off. Lysed cells were spun at 150,000 × g on an ultracentrifuge (Beckman) at 4° C for 75 minutes. The supernatant was passed through a 2 mL Ni-NTA Agarose (PerfectoPro, 5 Prime inc) column. The column was washed with 4 × 3 column volumes with wash buffer (50 mM Tris-HCl (pH 8), 200 mM NaCl, 50 mM imidazole). The protein was eluted off the column with 6 × 0.5 column volumes of elution buffer (50 mM Tris-HCl (pH 8), 200 mM NaCl, 500 mM imidazole). Elutions containing protein were collected and dialyzed 3 × 1 L in buffer (50 mM Tris-HCl (pH 8), 200 mM NaCl). The protein was stored at −80°C.

Isolation of membrane fractions containing WcfS

WcfS was isolated as above with a few minor changes. After sonication, lysed cells were homogenized on ice and centrifuged at 856 × g for 25 minutes. The supernatant was spun at 150,000 × g at 4° C for 75 minutes. The pellet, containing membrane components, was homogenized in 3mL of lysis buffer and stored at −80° C. Total protein concentration was 4.6 mg/mL, as determined by Bradford assay using BSA as a standard.

Detection of Recombinant Proteins

Purified protein was subjected to SDS-PAGE (10%) analysis for molecular weight confirmation and protein was detected by staining gels with Coomasie R-250. Protein was also transferred to nitrocellulose for Western Blot analysis. Nitrocellulose was stained with PonceauS to visualize all protein present. Nitrocellulose was then washed and blocked for at least four hours in 5% milk in PBS containing 0.05% Tween-20 (PBS-T) then were washed 3 X 15 min with PBS-T. Nitrocellulose containing proteins were incubated overnight with 1:3000 mouse anti-His antibody (GE Heathcare) or 1:10,000 anti-T7 antibody-linked to alkaline phosphatase (Pierce) diluted in PBS-T. Unbound antibody was removed with 3 X 15 min PBS-T washes. Blots were then incubated with 1:10,000 anti-mouse antibody linked to alkaline phosphatase (Pierce) four hours to overnight then washed as above. All proteins were detected using NBT/BCIP (Pierce).

Cross-linking studies on WcfR

WcfR was mixed with BS^3 crosslinking reagent (Pierce) as follows: 17 μM WcfR, 25 mM bicine (pH=8.5), 150 mM NaCl, 435 μM BS^3. Aliquots of 15 μL were removed from the solution at 0.5, 1, 4 and 8 minutes and mixed with 10 μL of 1.5 M Tris-HCl to quench the reaction. Samples were then loaded onto a 5% SDS-PAGE gel and analyzed by gelcode blue staining (Pierce).

Dynamic light scattering studies on WcfR

WcfR samples were dialyzed overnight in 25 mM bicine (pH=8.5)/150 mM NaCl. Small particulates were removed by centrifugation. Samples were then analyzed using standard methods for dynamic light scattering on a DynaPro NanoStar Light Scatterer at the MIT Bioinstrumentation facility.

Analytical separation of UDP-Sugars using HPLC

The separation of sugar standards, UDP-GlcNAc, UDP-AADGal, and UDP-4-keto sugar (ranging from 2.8–4.0 nmols), were separated by HPLC with an aminopropyl linked silane column (Agilent Zorbax NH_2 5 μm 4.6 × 250 mm) and column guard. Separations were performed for sugar analysis using 150 mM ammonium acetate at a flow rate of 2 mL/min at pH=4.5. The uridine ring of the sugar was detected by monitoring absorbance at 260 nm with 4 nm bandwidth.

Preparative Separation of UDP-Sugars

Preparative scale isolations of UDP-sugars were performed as described above with slight modifications. Preparative isolations used an isocratic method with 25–50 mM ammonium acetate, pH 4.5 (flow rate of 1 ml/min). UDP-sugars that were isolated using this method were dried overnight and the remaining acetate and other contaminants were removed by passing the sugars over a preparative scale C18 column (Varian 250 × 21.2 mm column) using 25 mM ammonium bicarbonate mobile phase (flow rate of 4 ml/min).

Analytical separations by Capillary Electrophoresis

Samples were filtered through spin concentrators (Millipore Centrifugal Filter Units) spun at 19,745 × g for 15 min and diluted with water 1:1. A 40 μL sample was loaded into 0.5 mL CE vials and loaded onto the system. The bare silica capillary (polymicro 49 μm × 45 cm) was washed with running buffer (100 mM borate (pH 9.15)) for 3 min before each analysis. Samples were introduced by pressure injection for 10 s at 0.5 psi, and the separation was performed at 15 kV. Reaction and standard components were monitored at 260 nm.

TLC analysis of bactoprenyl-linked reaction components

Reactions were prepared containing 1.4 nmols of NA-B-P synthesized as described previously (26) except using ammonium form isopentenyl dphoshpate, or 5 nmols of undecaprenol purchased from ARC, 20 μL of membrane fraction (92 μg of total protein) containing WcfS 1.5 nmols UDP-[^{3}H]AADGal (79 dpm/pmol), 50 mM TrisOAc (pH=8.0), 1% Triton-X-100, 10 mM $MgCl_2$, 1 mM ATP, 20 μL of membrane fraction containing *S. mutans* diacylglycerol kinase (transfers phosphate from ATP to undecaprenol providing *in situ* undecaprenyl phosphate (27)) in a total volume of 200 μL. Reactions were incubated at room temperature for 1 hour then 50 μL was quenched in 800 μL of 2:1 $CHCl_3$/MeOH. The organic layer was washed with 3 X 200 μL pure solvent upper phase (PSUP, 4% KCl in 1:1 methanol/water). The organic layer was dried under a stream of air and was redissolved in 200 μL of DMSO. Separately the organic and aqueous layers were diluted in 4.7 mL of ECOLITE scintillation fluid and were counted on a Perkin-Elmer Tricarb Scintillation counter. The percent turnover was calculated from the amount of tritium in each layer. Each reaction was performed in duplicate including controls that did not contain WcfS. The remaining reaction was extracted as described above and the organic layer was dried on a vacuum concentrator. The residue was dissolved in 50 μL of *n*-propanol then spotted on Whatman K6F TLC plates. Plates were resolved in 73/53/11 $CHCl_3$/MeOH/0.1 M NaBorate over 50 mm. Labeled product was then analyzed on a Bioscan AR-2000 radio-TLC imaging scanner. UDP-[^{3}H]AADGal was also spotted and analyzed through identical methods. In

addition, the origin and solvent front of the TLC plates were also spotted to ensure appropriate calibration of the imaging scanner position.

Reverse Phase HPLC analysis of bactoprenyl-linked reaction components

Reverse phase (RP) isocratic HPLC on bactoprenol-linked materials was performed on a C18 column (Agilent Eclipse XDB-C18 5μm 4.6 × 150mm) in 50% *n*-propanol/50% ammonium bicarbonate (25 mM). Products were purified using an isocratic method 75% *n*-propanol/25% ammonium bicarbonate (25 mM) on a C18 Varian 250 × 21.2 mm column (flow rate 4.0 ml/min).

Enzymatic Reactions of WcfR

WcfR function was analyzed with 2.6 nmols of standard UDP 4-keto sugar produced as described previously (15) with 15 mM L-glutamate and 100 μM pyridoxal 5'-phosphate (PLP) in 50mM Tris-acetate (pH=8) and 50mM NaCl and analyzed using CE. To synthesize UDP-AADGal, a two-step coupled reaction of WcfR and the characterized *C. jejuni* dehydratase, PglF, was used (15). The UDP-4-keto sugar was produced using the PglF conditions previously described by Olivier et al. with 0.64 mg of $PglF_{130}$ enzyme in a 1 mL solution. After 10 h, 0.16 mg of purified WcfR was added to the reaction solution along with 15 mM L-glutamate and 100 μM pyridoxal 5'-phosphate (PLP); the mixture was incubated for 4–6 h at 28° C. Reactions with PglF and WcfR were analyzed by CE then isolated and purified using HPLC. After vacuum concentrating, the UDP-AADGal sugar product was quantified spectrophotometrically.

Synthesis of UDP-[^{3}H]AADGal

UDP-[^{3}H]AADGal was synthesized using the two step reaction described above. A 100 μL reaction with 10 μL of UDP-[^{3}H]GlcNAc (8752 dpm/pmol), 0.33 μM UDP-GlcNAc, 25 μM NAD^+, 0.1% Triton-X-100, and 160 ng PglF was incubated for 6 h after which an additional 160 ng PglF was added and incubated at room temperature overnight. PLP 100 μM and L-glutamate 15 mM (final concentrations) were added along with 200 ng WcfR and incubated for 4 h at room temperature. After incubation the UDP-[^{3}H]AADGal was isolated using HPLC as described above.

Enzymatic Reactions of WcfS

The NA-B-PP-AADGal was prepared by adding 5 μL WcfS membrane fraction (23 μg of total protein) to a 200 μL solution containing 0.1 nmol NA-B-P *cis-6* or *cis-7*, 19.6 nmol UDP-AADGal, 1% Trition-X-100 hydrogenated, 10 mM $MgCl_2$, 0.5% DMSO, and 50 mM Tris-HCl. The reaction incubated at room temperature for 30 min, and was analyzed using the RP-HPLC method described above. Two negative controls one containing no WcfS and the other containing no UDP-AADGal were prepared for comparison.

Coupling of WcfR and WcfS

A 200 μL reaction was prepared as described above with the addition of 15 mM L-glutamate, 100 μM PLP, and 26 nmol UDP-4-keto sugar in the place of UDP-AADGal. To test the coupling of WcfR, WcfS, and PglF, a 200 μL reaction was prepared as described with the WcfR/WcfS reaction in addition to 25 μM NAD^+ and 33 nmol of UDP-GlcNAc. Controls in the absence of sugar were also prepared. The coupled reactions and controls were incubated for 30 min at room temperature and analyzed by HPLC.

Results

Isolation and biophysical characterization of WcfR

The reported structure of CPSA includes a rare α-linked acetamido-4-amino-6-deoxy-galactopyranose (AADGal). The biosynthesis of a nucleotide-linked-AADGal sugar (Scheme 1) has not been previously reported. However, two similar sugars, bacillosamine and 6-deoxy-4-amino-2-acetamido-*l*-altrose (AltNac, Figure 2), have been reported as products of the *C. jejuni* aminotransferases PglE and PseC respectively (15, 17). The CPSA biosynthesis gene locus in *B. fragilis* includes a proposed aminotransferase, WcfR, with 48% similarity to PglE, and PseC. The relatively low sequence similarity to well characterized aminotransferases prompted us to isolate WcfR for biochemical characterization. The gene encoding the predicted aminotransferase was amplified from *B. fragilis* genomic DNA and was incorporated into a pET-24a vector. The protein was expressed in *E.coli* BL-21(DE3) RIL cells and purified by Ni-NTA affinity chromatography. The presence of the recombinant protein was confirmed by Western Blot analysis (Supporting Figure 1). Greater than 16 mg of protein was isolated per liter of cell culture. Dynamic light scattering studies on the protein suggested that it was a monodispersed dimer consistent with similar proteins previously characterized (Supporting Figure 2) (28). Cross-linking studies using the water-soluble cross-linker BS^3 confirmed the presence of the dimer in solution (Supporting Figure 3).

WcfR catalyzes UDP-AADGal formation from a UDP-4-keto sugar

WcfR amino acid sequence analysis suggested that it was an aspartate aminotransferase (AAT) superfamily member that utilizes a pyridoxal 5’ phosphate (PLP) as an electron sink for transamination reactions. However, some AAT family members play a role in elimination, decarboxylation and racemization reactions (15, 17). To test the proposed function of the recombinant WcfR, a UDP-4-keto sugar (scheme 1) was required. Efforts to isolate the *B. fragilis* dehydratase UngD2, previously reported through genetic studies (12) to produce the WcfR substrate were unsuccessful. The *C. jejuni* protein PglF catalyzes the formation of a UDP-4-keto sugar with the appropriate stereochemistry at the 5” position from UDP-GlcNAc. To bypass the need of the *B. fragilis* enzyme and to determine if we could replace it with an enzyme from another organism, PglF was isolated and utilized to produce UDP-4-keto sugar as described previously (15). Purified WcfR was incubated with the UDP-4-keto sugar, PLP, and L-glutamate. Product formation was then analyzed by capillary electrophoresis (CE) (Figure 3). The UDP-4-keto sugar was over 90% consumed by WcfR to give a new peak with less electrophoretic mobility, which was consistent with the addition of an amino group. These results suggest that WcfR is the aminotransferase required for the biosynthesis of the AADGal sugar in CPSA.

Amine resin based isolation of UDP-linked sugars

Identifying the location of the incorporated amine in the UDP-AADGal sugar required a robust isolation method. A variety of methods are available for HPLC separation of UDP-sugars including reverse phase (RP) on C18 with ion-pairing agents like triethylammonium bicarbonate (TEAB) and RP coupled to ion exchange methods using phosphate buffers (15, 29–34). However, in our hands we were unable to separate similar sugars using the TEAB methods, and for further characterization we were interested in utilizing a volatile buffer system rather than phosphate. A column consisting of an aminopropylsilane provided reproducible HPLC separations that could be easily controlled by pH or ammonium acetate buffer concentration. Of particular interest was the large difference in retention between the UDP-4-keto sugar and UDP-AADGal as shown in Figure 4. Note that the chromatogram shown in Figure 4 is the midpoint of a PglF/WcfR coupled reaction described below. The use of the aminopropysilane column provided excellent separation of the reaction

components and may provide a novel method for the separation of other similar UDP-sugars.

Characterization of UDP-AADGal

The unusual stereoconfiguration and identity of the UDP-AADGal isolated by HPLC was determined through a series of spectroscopic studies. The expected molecular weight of UDP-AADGal (589.1 amu) was confirmed by negative ion mode ESI-MS as shown in Figure 5, where only the -1 ion was detected. High resolution MS analysis further demonstrated the expected molecular weight of the product and the insertion of an amine in the sugar structure (Supporting Figure 4). Proton decoupled ^{31}P-NMR (Supporting Figure 5) analysis suggested the presence of the linking diphosphate moiety, and J coupling values (Table 1) of the clear phosphorous doublets were consistent with previously characterized UDP-sugars (15, 17, 35). Analysis by 1D ^{1}H-NMR (Figure 5) was used for structural characterization with 2D correlation spectroscopy (COSY, Supporting Figure 6) to independently assign the spectrum. The chemical shifts and COSY correlations are provided in Table 1 for the entire UDP-sugar. Using the COSY spectrum we were able to assign each peak of the pyranose ring, and found the chemical shifts to be consistent with similar sugars from other bacterial systems (Supporting Table 2) (15, 17, 35). However, the COSY and ^{1}H-NMR spectra could not provide stereochemical information on the product.

Stereoconfiguration of UDP-AADGal

In order to characterize the stereochemical configuration of UDP-AADGal we used phase dependent Transverse Rotating-frame Overhauser Enhancement Spectroscopy (T-ROESY, Supporting Figure 7). This NMR technique allowed the detection of clear through space interactions and the magnitude of those interactions between each of the pyranose ring protons (Table 1). We observed a relatively strong interaction between the H1” and H2” protons (Figure 5) as determined by integral magnitude (Table 1). However, the magnitude of the integral for a cross-peak between H2” and H3” was very weak, suggesting these were on opposite sides of the sugar. There was a strong correlation (>5 integral units) between the H3”/H4”, H4”/H5”, and H5”/H3” suggesting that all of these protons were on the same side of the pyranose ring. There was a relatively weak through space interaction associated with the H4”/H6” crosspeak, suggesting some proximity between the C6” methyl group and the equatorial H4”. As expected there was also a strong correlation between the H5” and the C6” methyl protons. All together these results strongly support the proposed stereoconfiguration of the novel UDP-AADGal sugar, which is identical to the unlinked sugar previously described in CPSA (36).

Similarity of WcfS to a known initiating hexose-1-phosphate transferase

Initiating hexose-1-phosphate transferases link phopho-sugars from UDP-linked sugars to bactoprenyl phosphate (B-P) scaffolds. The similarity of the AADGal sugar to the characterized di-N-Ac-Bacillosamine of *C. jejuni* prompted us to assume that the AADGal was the first sugar to be incorporated into the bactoprenyl scaffold in CPSA biosynthesis (Scheme 1) (37–39). Of the four proposed glycosyltransferases present in the CPSA biosynthesis gene locus, one gene had similarity to the initiating hexose-1-phosphate transferase from *C. jejuni*, PglC. The protein encoded by the *wcfS* gene was 41% identical and 60% similar to the *C. jejuni* initiating hexose-1-phosphate transferase suggesting that the WcfS protein may transfer the AADGal sugar phosphate to bactoprenyl phosphate.

WcfS Expression

In order to test the function of WcfS, the gene encoding the predicted initiating hexose-1-phosphate transferase was amplified by PCR and incorporated into a pET-24a vector that

encoded a C-terminal hexahistidine tag. Plasmid encoding WcfS was transformed into BL-21 (DE3) RIL cells and protein was expressed using auto-induction. WcfS was predicted to contain one transmembrane domain by the TMHMM prediction software (Supporting Figure 8) (40). WcfS could be functionally isolated in the membranes of the *E. coli* expression cells. Western Blot analysis was used to confirm the presence of the recombinant protein in the membrane fraction (Supporting Figure 1). It is important to note that the WcfS protein was ligated into a pET-24a vector that did not include an N-terminal T7-tag coding sequence. As expected the WcfS protein was not detected using an anti-T7 antibody, but was detected using the anti-His antibody.

WcfS catalyzes the transfer of [^{3}H]AADGal to bactoprenyl phosphate

WcfS was thought to link phospho-AADGal to bactoprenyl phosphate. To test the function of WcfS, we first synthesized a radiolabeled UDP-[^{3}H]AADGal from UDP-[^{3}H]GlcNAc, as described above with unlabeled material. The product of this reaction was characterized by RP-HPLC analysis and comparison with an authentic unlabeled product. Specific activity was calculated from the UV absorbance of the uridine ring at 260 nm and the tritium count of the purified UDP-[^{3}H]AADGal. Using the method of Hartley, Larkin and Imperiali (27), undecaprenyl phosphate was produced from commercially available plant undecaprenol and *S. mutans* diacylglycerol kinase which has been shown to monophosphorylate undecaprenol. The reaction solution was then mixed with UDP-[^{3}H]AADGal and WcfS containing membrane fraction (Scheme 1). The organic soluble undecaprenyl-linked product was next isolated by organic/aqueous extraction. We found, as shown in Figure 6a, that the presumed initiating hexose-1-phosphate transferase, WcfS, could transfer the water soluble [^{3}H]AADGal to the organic soluble undecaprenol.

Reaction of bactoprenyl analogues in WcfS catalyzed reactions

Previously our group has described the use of a *p*-nitro-aniline bactoprenyl phosphate (NA-B-P, Figure 7) analogue with the WcfS homologue PglC from *C. jejuni* (26). This analogue provided significant advantages over reactions with undecaprenol in that it could be readily detected by HPLC and TLC analysis, which would allow for simple isolation of very small quantities of product without the use of expensive radiolabels. To initially test the activity of the analogue, WcfS membrane fraction and UDP-[^{3}H]AADGal was mixed with NA-B-P *cis-7*. By extraction analysis, as above, transfer of tritium was observed to the organic soluble NA-B-P, as shown in Figure 6a. TLC analysis of the NA-B-P and undecaprenol reactions revealed a new radioactive material with similar retention factors formed in both reactions, as shown in Figure 6b. Radiolabel was incorporated into a product with mobility drastically increased from the UDP-[^{3}H]AADGal substrate. Separately in larger scale reactions, we observed a light yellow spot with the same retention factor observed with the radioactive samples. These results strongly suggested that WcfS did catalyze transfer of phospho-AADGal to the analogue. Control reactions with WcfS replaced with only kinase membrane fraction did not result in altered mobility of the reactants.

HPLC isolation of bactoprenyl-linked AADGal

Utilizing undecaprenol as a substrate for initiating hexose-1-phosphate transferases makes it difficult to isolate modified product as there is no easily distinguishable chromophore associated with the molecule. However, the *p-nitro-aniline* moiety on NA-B-P is easily distinguishable spectrophotometrically. We took advantage of this property of the analogue to test the activity of NA-B-P of different lengths (Figure 7) with WcfS. Reactions were prepared with unlabeled UDP-AADGal in excess of NA-B-P *cis-6* or *cis-7* (26). Product retention times were clearly distinguishable by RP-HPLC in 50% *n*PrOH/ammonium bicarbonate and there was a decrease in retention with the increased polarity of the phospho-AADGal, as shown in Figure 8a–b. We found that NA-B-P with both six and seven *cis*

isoprene additions were substrates for WcfS. However, the turnover for the NA-B-P *cis-7* (78%) isoprenoid was slightly lower than with the *cis-6* (~90%) isoprenoid. these results were consistent with previous studies by the Walker group with multiple length isoprenes, and is presumably due to the increase in micelle formation with the longer chain isoprenoids (41). Product was isolated from the NA-B-P *cis-6* reaction and the identity of the new product was confirmed by high resolution MS analysis (Supporting Figure 9).

PglF, WcfR and WcfS can be coupled for a single pot synthesis of bactoprenyl diphosphate-AADGal

A major advantage to the use of enzymes in the biosynthesis of complex oligosaccharides is the selectivity of these proteins for specific substrates. We were interested in whether this could be taken advantage of to biosynthesize the bactoprenyl diphosphate-linked monosaccharide in a single pot reaction. First, PglF and WcfR were tested to determine if they could be readily coupled to give UDP-AADGal without isolation of the UDP-4-keto sugar. The results from the two-step reaction showed excellent turnover to the expected UDP-AADGal product. Figure 4 shows an intermediate timed reaction in which HPLC peaks are observed for the UDP-GlcNAc, UDP-4-keto sugar and UDP-AADGal. Reactions were also prepared containing WcfS, WcfR, NA-B-P *cis-7* and the UDP-4-keto sugar. We found that there was full conversion to the monosaccharide product in this reaction, as shown in Figure 9a. Next reactions were prepared containing WcfS, WcfR, PglF with no sugar substrate or with UDP-GlcNAc. In the presence of all three proteins, substrates and cofactors with UDP-GlcNAc, conversion to bactoprenyl diphosphate-linked product was observed (Figure 9b). These results demonstrate that all of the enzymes in this system can be coupled for the formation of the first CPSA bactoprenyl-linked sugar in a single pot reaction.

Discussion

In this report we have taken the first critical step in the *in vtiro* assembly of CPSA, a complex sugar polymer that has been shown to have therapeutic potential for Inflammatory Bowel Disease as well as Multiple Sclerosis (3, 5). We have shown that the AADGal sugar can be readily formed using a combination of enzymes from *C. jejuni* and the native organism *B. fragilis*. We have also demonstrated the role of the initiating hexose-1-phosphate transferase, WcfS, which catalyzes the addition of AADGal to bactoprenol. There are three additional glycosyltransferase genes associated with the *B. fragilis* CPSA biosynthesis locus, *wcfN, wcfP* and *wcfQ*. Here we have for the first time used a bactoprenyl phosphate probe to interrogate the first enzyme in this pathway, and will be able to utilize the product from these reactions to readily identify the role of the remaining glycosyltransferases.

The AADGal stereochemistry has been reported in the native CPSA polysaccharide (36), and we have clearly demonstrated that this sugar can be synthesized with WcfR, and transferred to bactoprenyl phosphate by WcfS. However, it is possible that these enzymes could also utilize the previously characterized bacillosamine and *l*-AltNAc 4-amino sugars (Figure 2). It would be of great interest to determine the preferred substrate stereochemistry of the WcfR and WcfS proteins. In addition, the dehydratase responsible for biosynthesizing the substrate for WcfR has not been previously isolated. Work by the Comstock group has suggested that the dehydratase is encoded by the gene *ungD2* (12). However, in our hands we have not been able to demonstrate this function from the protein encoded by the *ungD2* gene as of yet. The biochemical role of this gene is of great importance and is the subject of future work by our group.

The lack of a dehydratase in the CPSA biosynthesis locus required us to use the previously characterized soluble PglF from *C. jejuni* to provide the substrate needed to test WcfR function. It was interesting that we observed coupling with the soluble PglF and WcfR, since coupling was only observed with full length PlgF and the aminotransferase PglE in the *C. jejuni* Pgl pathway (15). Crucially, it was of considerable interest that enzymes coupled from different organisms provided a function that was not readily observed from the native organism proteins *in vitro*. We have also shown in this report that a single pot synthesis can be utilized for the biosynthesis of the first bactoprenyl diphosphate-linked monosaccharide using PglF, WcfR and WcfS. One of the ultimate goals of our work is to produce CPSA. In fulfilling that goal it would be ideal if we could couple as many enzymes as possible for the biosynthesis of this complex polysaccharide.

The unusual stereochemistry of the UDP-AADGal sugar prompted concern over the identity of the sugar produced by WcfR. UDP-4-amino sugar biosynthesis, similar to AADGal, has been characterized in a number of systems (15–17, 35). Comparison of our NMR data and the data obtained on the previously characterized UDP-sugars (Supporting Table 2) strongly suggests that the sugar synthesized in this work is UDP-AADGal. The similar UDP-bacillosamine (UDP-Bac, Figure 2) differs only in the stereochemistry of the 4”-amino group. Remarkably, proton peaks in the sugar reported here were identical (within 0.1 ppm) to UDP-Bac, except the chemical shifts associated with the H3”, H4” and H5” of the pyranose ring. The H3”, H4” and H5” were all shifted downfield 0.29, 0.49 and 0.24 ppm respectively relative to UDP-Bac (17). It is very important to note that the position where the stereochemistry is flipped in UDP-AADGal had the largest chemical shift difference. In addition, the *l*-AltNAc sugar (Figure 2) has the same stereochemistry as our 4-amino sugar at the H4” position, but differs at H5”. Between these two sugars, we observe the most significant differences in chemical shift in the H4” and H5” with 0.17 and 0.32 ppm difference in each respectively. The largest shift difference again was between the UDP-AADGal and UDP-AltNAc sugar at the position which corresponded to the difference in stereochemistry. In addition to the phase dependent T-ROESY results described above the consistency with the previously characterized sugars strongly suggests the correct assignment of stereochemistry in this report. Interestingly, there is one report on the biosynthesis of an AADGal type of sugar (35). However, later analysis of the activity of the same biosynthetic protein responsible for this sugar suggested that it actually had the *l*-AltNAc stereochemistry (17). In addition, the authors of the former report note a strong NOE between the H1” and H5” of the pyranose ring consistent with the *l*-AltNAc 4-amino sugar stereochemistry.

The CSPA tetrasaccharide repeating unit has been characterized (36). It has been suggested that AADGal was the initial sugar linked to a bactoprenyl membrane scaffold in a Wzy dependent pathway for biosynthesis of the sugar polymer (12). The genes *wcfR* and *wcfS* were proposed to encode an aminotransferase and initiating hexose-1-phosphate transferase involved in linking phospho-AADGal to bactoprenyl phosphate (13). In this work we were able to demonstrate that WcfR exhibits aminotransferase activity and WcfS acts as an initiating hexose-1-phosphate transferase for attachment of AADGal to an isoprenid-linked membrane scaffold. In doing this we developed a method of separating UDP-linked sugars and found that the aminotransferase, WcfR produces a UDP-4-amino sugar with unreported stereochemistry. We were also able to couple WcfR and WcfS with a dehydratase from a different organism to produce the lipid-linked AADGal in a single pot reaction. In addition, using our previously described bactoprenyl analogue, progress of isoprenoid utilizing enzyme reactions could be readily monitored and products could be isolated. This work demonstrates a key step to a fully *in vitro* biosynthetic route to producing the potentially therapeutic CPSA from *B. fragilis*.

Supplementary Material

Refer to Web version on PubMed Central for supplementary material.

Acknowledgments

Funding Sources

This work was supported by NIH AREA grant R15GM100402 (JMT)

We thank Dr. Barbara Imperiali for PglF and *S. mutans* kinase expressing cells, Dr. Jian Liu for allowing us to use his MS system and for training, Dr. Michael Murphy and Richard Hardin for help with NMR data collection and processing, Dr. Brian Cooper for help with CE, Dave Hometchko for help with HPLC method development, Christina Martinez for synthesis of NAGPP, Sunita Sharma for early expressions of WcfS, Donovan Lujan for expression of WcfR, and Dr. Angelyn Larkin for critical reading of the manuscript and helpful suggestions.

ABBREVIATIONS

CPSA	Capsular Polysaccharide A
AADGal	acetamido-4-amino-6-deoxy-galactopyranose
CE	Capillary Electrophoresis
HPLC	high performance liquid chromatography
ESI-MS	electrospray ionization Mass Spectrometry
NMR	Nuclear Magnetic Resonance
TLC	Thin layer chromatography
NA-B-P	*p*-nitroaniline bactoprenol
WcfR	an aminotransferase
PlgF	a dehydratase
WcfS	an initiating hexose-1-phosphate transferase
FPP	farnesyldiphosphate
IPP	isopentenyl diphosphates
PCR	Polymerase Chain Reaction
UDP	Uridine diphosphate
GlcNAc	*N*-Acetylglucosamine
GalNAc	N-Acetylgalactoamine
PLP	pyridoxal 5’-phosphate
TEAB	triethyl ammonium bicarbonate, cef, cell envelope fraction (cef)
COSY	Correlation spectroscopy
NOSEY	Nuclear Overhauser effect spectroscopy
T-ROSEY	Transverse Rotating-frame Overhauser Enhancement Spectroscopy

References

1. Tremaroli V, Backhed F. Functional interactions between the gut microbiota and host metabolism. Nature. 2012; 489:242–249. [PubMed: 22972297]

2. Maynard CL, Elson CO, Hatton RD, Weaver CT. Reciprocal interactions of the intestinal microbiota and immune system. Nature. 2012; 489:231–241. [PubMed: 22972296]

3. Surana NK, Kasper DL. The yin yang of bacterial polysaccharides: lessons learned from B. fragilis PSA. Immunological Reviews. 2012; 245:13–26. [PubMed: 22168411]

4. Chung HC, Kasper DL. Microbiota-stimulated immune mechanisms to maintain gut homeostasis. Current Opinion in Immunology. 2010; 22:455–460. [PubMed: 20656465]

5. Ochoa-Reparaz J, Mielcarz DW, Wang Y, Begum-Haque S, Dasgupta S, Kasper DL, Kasper LH. A polysaccharide from the human commensal Bacteroides fragilis protects against CNS demyelinating disease. Mucosal immunology. 2010; 3:487–495. [PubMed: 20531465]

6. Cobb BA, Wang Q, Tzianabos AO, Kasper DL. Polysaccharide processing and presentation by the MHCII pathway. Cell. 2004; 117:677–687. [PubMed: 15163414]

7. Mazmanian SK, Kasper DL. The love-hate relationship between bacterial polysaccharides and the host immune system, Nature reviews. Immunology. 2006; 6:849–858. [PubMed: 17024229]

8. Mazmanian SK, Liu CH, Tzianabos AO, Kasper DL. An immunomodulatory molecule of symbiotic bacteria directs maturation of the host immune system. Cell. 2005; 122:107–118. [PubMed: 16009137]

9. Pragani R, Seeberger PH. Total synthesis of the Bacteroides fragilis zwitterionic polysaccharide A1 repeating unit. Journal of the American Chemical Society. 2011; 133:102–107. [PubMed: 21142035]

10. Pragani R, Stallforth P, Seeberger PH. De novo synthesis of a 2-acetamido-4-amino-2,4,6-trideoxy-D-galactose (AAT) building block for the preparation of a Bacteroides fragilis A1 polysaccharide fragment. Organic letters. 2010; 12:1624–1627. [PubMed: 20196573]

11. Kalka-Moll WM, Tzianabos AO, Wang Y, Carey VJ, Finberg RW, Onderdonk AB, Kasper DL. Effect of molecular size on the ability of zwitterionic polysaccharides to stimulate cellular immunity. J Immunol. 2000; 164:719–724. [PubMed: 10623815]

12. Coyne MJ, Chatzidaki-Livanis M, Paoletti LC, Comstock LE. Role of glycan synthesis in colonization of the mammalian gut by the bacterial symbiont Bacteroides fragilis. Proceedings of the National Academy of Sciences of the United States of America. 2008; 105:13099–13104. [PubMed: 18723678]

13. Coyne MJ, Tzianabos AO, Mallory BC, Carey VJ, Kasper DL, Comstock LE. Polysaccharide biosynthesis locus required for virulence of Bacteroides fragilis. Infection and immunity. 2001; 69:4342–4350. [PubMed: 11401972]

14. Comstock LE, Coyne MJ, Tzianabos AO, Pantosti A, Onderdonk AB, Kasper DL. Analysis of a capsular polysaccharide biosynthesis locus of Bacteroides fragilis. Infection and immunity. 1999; 67:3525–3532. [PubMed: 10377135]

15. Olivier NB, Chen MM, Behr JR, Imperiali B. In vitro biosynthesis of UDP-N,N'-diacetylbacillosamine by enzymes of the Campylobacter jejuni general protein glycosylation system. Biochemistry. 2006; 45:13659–13669. [PubMed: 17087520]

16. Creuzenet C, Lam JS. Topological and functional characterization of WbpM, an inner membrane UDP-GlcNAc C6 dehydratase essential for lipopolysaccharide biosynthesis in Pseudomonas aeruginosa. Molecular microbiology. 2001; 41:1295–1310. [PubMed: 11580835]

17. Schoenhofen IC, McNally DJ, Vinogradov E, Whitfield D, Young NM, Dick S, Wakarchuk WW, Brisson JR, Logan SM. Functional characterization of dehydratase/aminotransferase pairs from Helicobacter and Campylobacter: enzymes distinguishing the pseudaminic acid and bacillosamine biosynthetic pathways. The Journal of biological chemistry. 2006; 281:723–732. [PubMed: 16286454]

18. Yother J. Capsules of Streptococcus pneumoniae and other bacteria: paradigms for polysaccharide biosynthesis and regulation. Annual review of microbiology. 2011; 65:563–581.

19. Woodward R, Yi W, Li L, Zhao GH, Eguchi H, Sridhar PR, Guo HJ, Song JK, Motari E, Cai L, Kelleher P, Liu XW, Han WQ, Zhang WP, Ding Y, Li M, Wang PG. In vitro bacterial polysaccharide biosynthesis: defining the functions of Wzy and Wzz. Nature Chemical Biology. 2010; 6:418–423.

20. Han WQ, Wu BL, Li L, Zhao GH, Woodward R, Pettit N, Cai L, Thon V, Wang PG. Defining Function of Lipopolysaccharide O-antigen Ligase WaaL Using Chemoenzymatically Synthesized Substrates. Journal of Biological Chemistry. 2012; 287:5357–5365. [PubMed: 22158874]
21. Whitfield C. Biosynthesis and assembly of capsular polysaccharides in Escherichia coli. Annual Review of Biochemistry. 2006; 75:39–68.
22. Whitfield C, Paiment A. Biosynthesis and assembly of Group 1 capsular polysaccharides in Escherichia coli and related extracellular polysaccharides in other bacteria. Carbohydrate research. 2003; 338:2491–2502. [PubMed: 14670711]
23. Nielsen P, Krogh A. Large-scale prokaryotic gene prediction and comparison to genome annotation. Bioinformatics. 2005; 21:4322–4329. [PubMed: 16249266]
24. Rodriguez-Ortega MJ, Luque I, Tarradas C, Barcena JA. Overcoming function annotation errors in the Gram-positive pathogen Streptococcus suis by a proteomics-driven approach. BMC Genomics. 2008; 9:588. [PubMed: 19061494]
25. Studier FW. Protein production by auto-induction in high density shaking cultures. Protein expression and purification. 2005; 41:207–234. [PubMed: 15915565]
26. Lujan DK, Stanziale JA, Mostafavi AZ, Sharma S, Troutman JM. Chemoenzymatic synthesis of an isoprenoid phosphate tool for the analysis of complex bacterial oligosaccharide biosynthesis. Carbohydrate research. 2012; 359:44–53. [PubMed: 22925763]
27. Hartley MD, Larkin A, Imperiali B. Chemoenzymatic synthesis of polyprenyl phosphates. Bioorganic & medicinal chemistry. 2008; 16:5149–5156. [PubMed: 18374576]
28. Larkin A, Olivier NB, Imperiali B. Structural Analysis of WbpE from Pseudomonas aeruginosa PAO1: A Nucleotide Sugar Aminotransferase Involved in O-Antigen Assembly. Biochemistry. 2010; 49:7227–7237. [PubMed: 20604544]
29. Carrey EA, Smolenski RT, Edbury SM, Laurence A, Marinaki AM, Duley JA, Zhu L, Goldsmith DJ, Simmonds HA. Origin and characteristics of an unusual pyridine nucleotide accumulating in erythrocytes: positive correlation with degree of renal failure. Clinica chimica acta; international journal of clinical chemistry. 2003; 335:117–129.
30. Cataldi TR, Campa C, De Benedetto GE. Carbohydrate analysis by high-performance anion-exchange chromatography with pulsed amperometric detection: the potential is still growing. Fresenius' journal of analytical chemistry. 2000; 368:739–758. [PubMed: 11227559]
31. Dorion S, Rivoal J. Quantification of uridine 5'-diphosphate (UDP)-glucose by high-performance liquid chromatography and its application to a nonradioactive assay for nucleoside diphosphate kinase using UDP-glucose pyrophosphorylase as a coupling enzyme. Analytical biochemistry. 2003; 323:188–196. [PubMed: 14656524]
32. Pieslinger AM, Hoepflinger MC, Tenhaken R. Nonradioactive enzyme measurement by high-performance liquid chromatography of partially purified sugar-1-kinase (glucuronokinase) from pollen of Lilium longiflorum. Analytical biochemistry. 2009; 388:254–259. [PubMed: 19272347]
33. Tomiya N, Ailor E, Lawrence SM, Betenbaugh MJ, Lee YC. Determination of nucleotides and sugar nucleotides involved in protein glycosylation by high-performance anion-exchange chromatography: sugar nucleotide contents in cultured insect cells and mammalian cells. Analytical biochemistry. 2001; 293:129–137. [PubMed: 11373089]
34. Yang T, Bar-Peled M. Identification of a novel UDP-sugar pyrophosphorylase with a broad substrate specificity in Trypanosoma cruzi. The Biochemical journal. 2010; 429:533–543. [PubMed: 20482518]
35. Obhi RK, Creuzenet C. Biochemical characterization of the Campylobacter jejuni Cj1294, a novel UDP-4-keto-6-deoxy-GlcNAc aminotransferase that generates UDP-4-amino-4,6-dideoxy-GalNAc. The Journal of biological chemistry. 2005; 280:20902–20908. [PubMed: 15790564]
36. Baumann H, Tzianabos AO, Brisson JR, Kasper DL, Jennings HJ. Structural elucidation of two capsular polysaccharides from one strain of Bacteroides fragilis using high-resolution NMR spectroscopy. Biochemistry. 1992; 31:4081–4089. [PubMed: 1567854]
37. Glover KJ, Weerapana E, Chen MM, Imperiali B. Direct biochemical evidence for the utilization of UDP-bacillosamine by PglC, an essential glycosyl-1-phosphate transferase in the Campylobacter jejuni N-linked glycosylation pathway. Biochemistry. 2006; 45:5343–5350. [PubMed: 16618123]

38. Weerapana E, Glover KJ, Chen MM, Imperiali B. Investigating bacterial N-linked glycosylation: synthesis and glycosyl acceptor activity of the undecaprenyl pyrophosphate-linked bacillosamine. Journal of the American Chemical Society. 2005; 127:13766–13767. [PubMed: 16201778]

39. Glover KJ, Weerapana E, Imperiali B. In vitro assembly of the undecaprenylpyrophosphate-linked heptasaccharide for prokaryotic N-linked glycosylation. Proceedings of the National Academy of Sciences of the United States of America. 2005; 102:14255–14259. [PubMed: 16186480]

40. Krogh A, Larsson B, von Heijne G, Sonnhammer EL. Predicting transmembrane protein topology with a hidden Markov model: application to complete genomes. J Mol Biol. 2001; 305:567–580. [PubMed: 11152613]

41. Perlstein DL, Zhang Y, Wang TS, Kahne DE, Walker S. The direction of glycan chain elongation by peptidoglycan glycosyltransferases. Journal of the American Chemical Society. 2007; 129:12674–12675. [PubMed: 17914829]

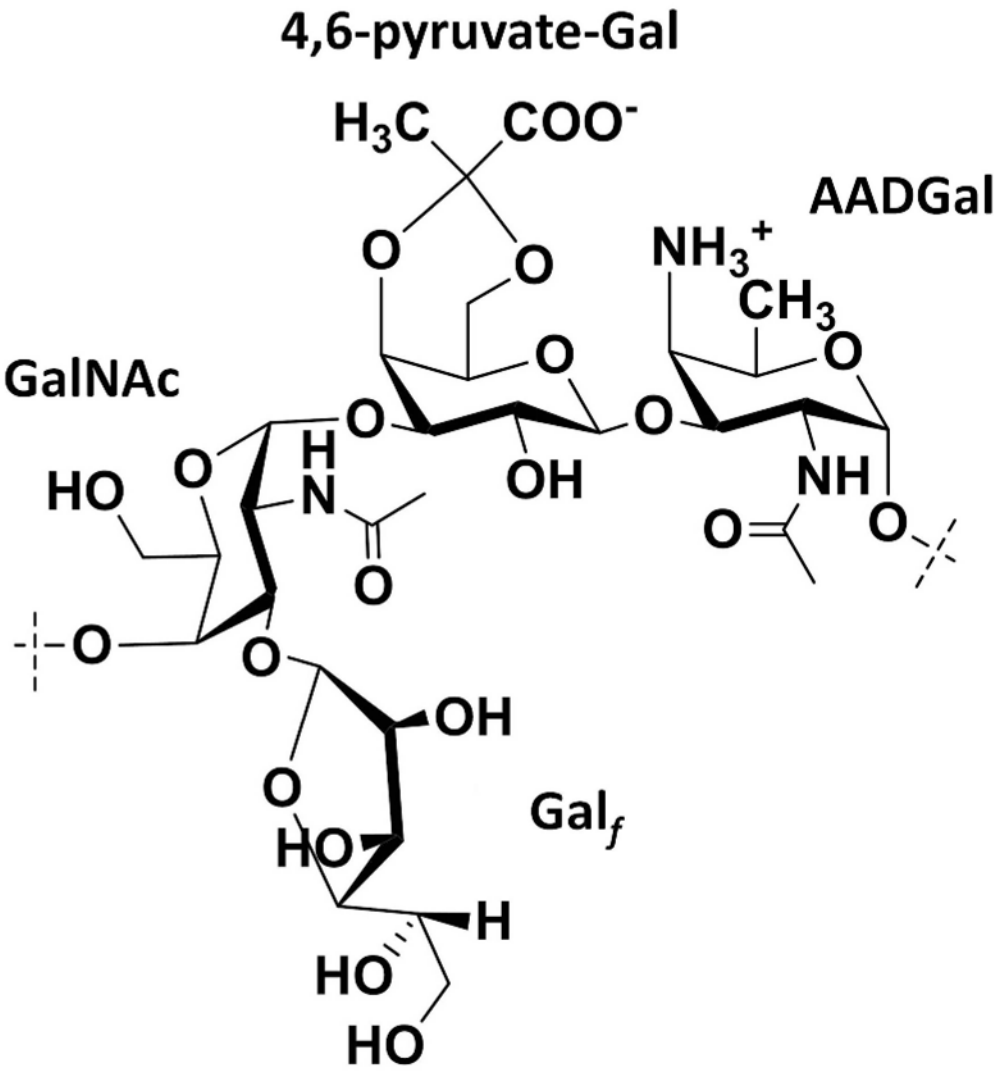

Figure 1. Capsular polysaccharide A repeat unit

CPSA repeat unit is made up of an acetamido-4-amino-6-deoxygalactopranose (AADGal), 4,6-pyruvate galactose (4,6-pyr-Gal), N-acetylgalactosamine (GalNAc), and a Galactofuranose (Gal_f) sugar. Dotted lines represent polymer linkage points AADGal--GalNAc

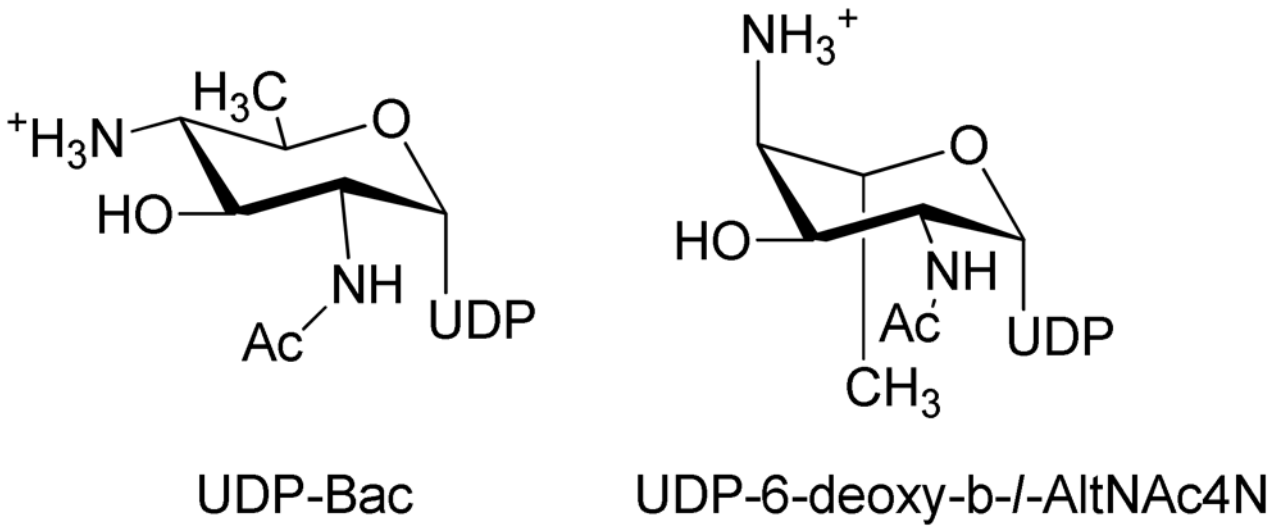

Figure 2.
Previously characterized UDP-linked 6-deoxy-4-amino sugars

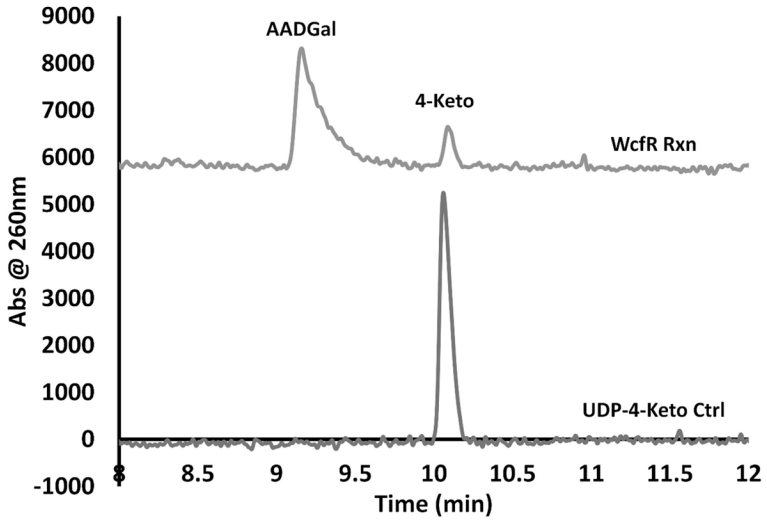

Figure 3. Capillary electrophoresis analysis confirms function of WcfR

CE analysis of the 0.33 mM UDP-4-keto sugar standard isolated from PglF and a WcfR reaction where 0.33mM UDP-4-keto sugar in the presence of 0.08 mg of WcfR, PLP, and L-Glutamate.

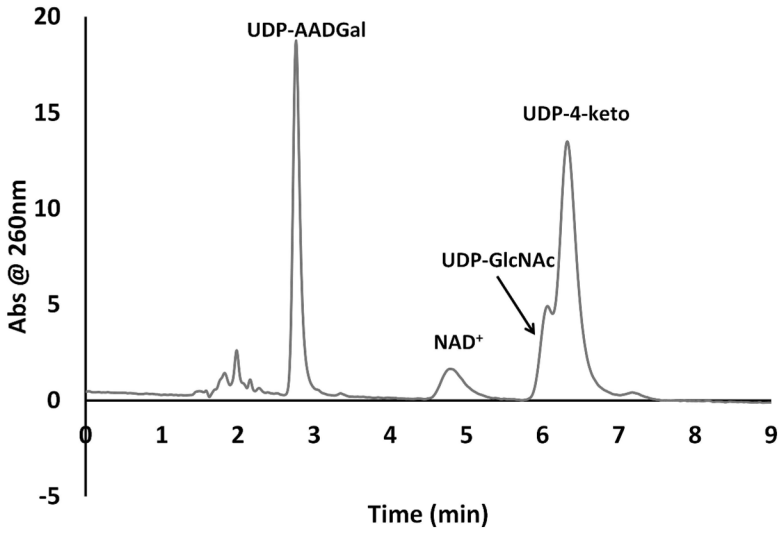

Figure 4. HPLC isolation of UDP-linked sugars on aminopropyl silane resin

a) HPLC analysis of the PlgF/WcfR coupled reaction with 0.33mM UDP-GlcNAc with 0.1 mg PglF and 0.08 mg WcfR in the presence of NAD+, PLP, and L-Glutamate. Run with 150mM ammonium acetate at a flow rate of 2mL/min at pH=4.5.

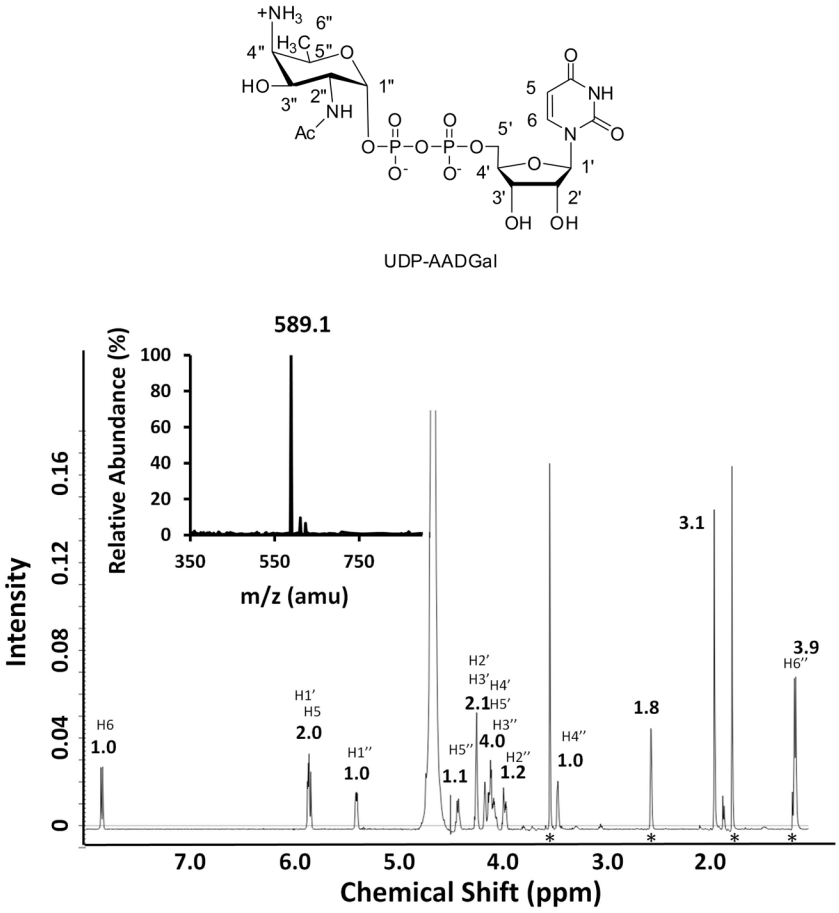

Figure 5. Characterization of the UDP-AADGal product of WcfR

^{1}H-NMR including carbon designations, assignments and integrals of each peak. Inset is the (−)ESI-MS spectrum showing a single peak with expected molecular weight 589.1.* indicates contaminant.

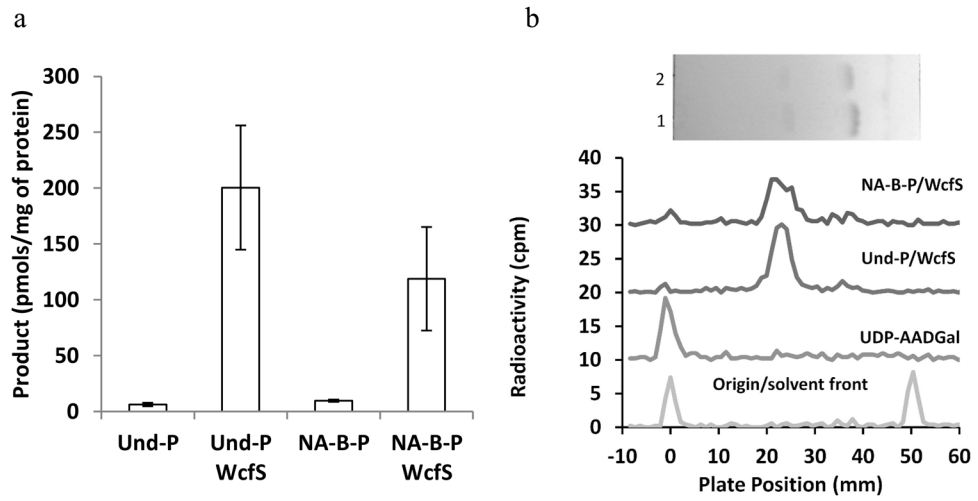

Figure 6. WcfS utilization of UDP-AADGal, Undecaprenol and NA-B-P *cis-7*

a) Reactions containing 5 nmols of UndOH or 1.4 nmols NA-B-P *cis-7* were mixed with 92 μg total protein WcfS membrane fraction and 1.5 nmols UDP-[^{3}H]AADGal. A 20 μL aliquot of product was extracted into $CHCl_3$ and washed with Pure Solvent Upper Phase. Organic and aqueous phases were counted on a scintillation counter. Percent incorporation was calculated by the amount of radiolabel in the organic layer relative to the total, and converted to pmols of product per μg of total protein in the reaction. b) TLC analysis of the dried remaining reaction from organic extractions on TLC plate scanner. Origin/solvent front) origin and solvent front markers for calibration, UDP-AADGal) sugar alone, Und-P/WcfS) WcfS reaction with UndOH, NA-B-P/WcfS) WcfS reaction with analogue. TLC plate shown is a 1) NA-B-P *cis-7* and 2) NA-B-P *cis-6* large scale reaction product with WcfS and UDP-AADGal. TLC plate is contrast enhanced to aid visualization.

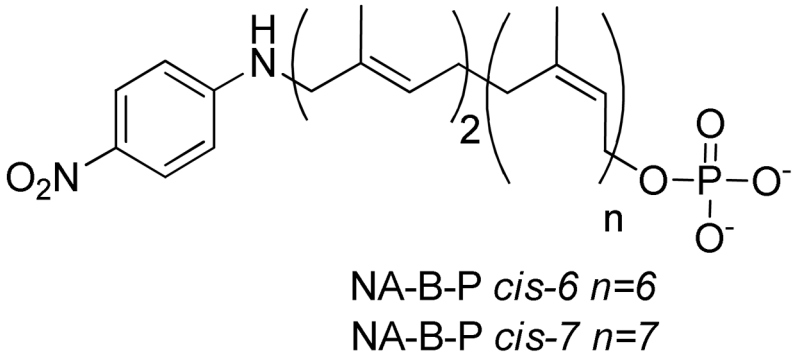

Figure 7. NA-B-P analogue

cis-6 and *cis-7* represent analogues with 6 and 7 *z*-configuration isoprenes respectively

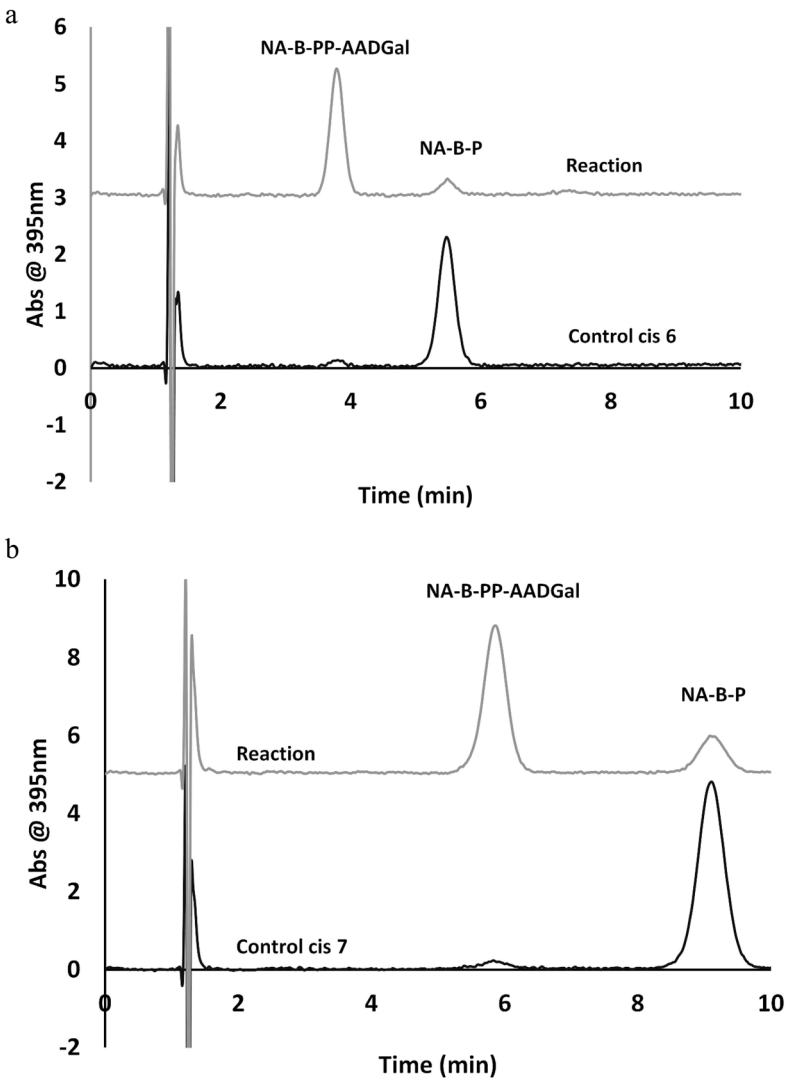

Figure 8. WcfS utilizes both *cis-6* and *cis-7* NA-B-P

a) HPLC analysis of a control of 23 μg total protein WcfS membrane fraction in the presence of a 20μM NA-BP and no UDP-linked sugar. The reaction contained the same amount of protein and analogue with 0.14 mM UDP-AADGal sugar. b) Analysis of a reaction identical to (a) except with NA-B-P *cis-7*.

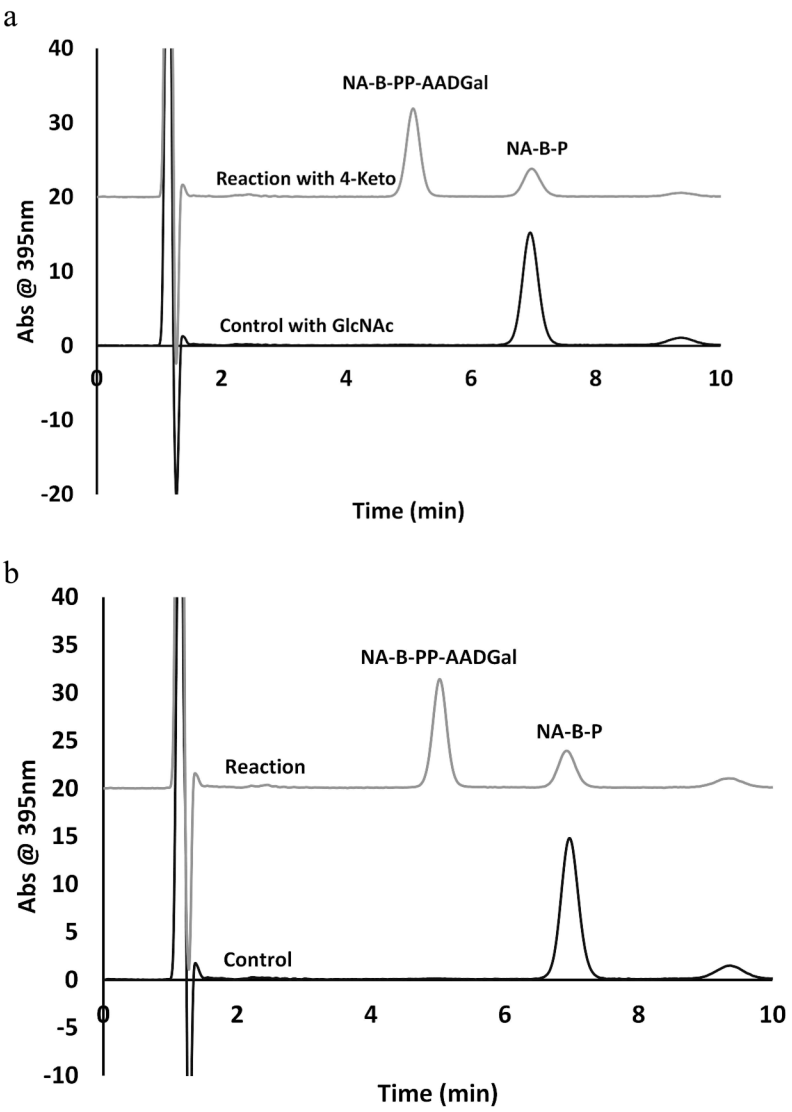

Figure 9. Single pot biosynthesis of NA-B-PP-AADGal

a) analysis in 1:1 PrOH/ammounium bicarbonate on C18 of a reaction containing 0.08mg WcfR and 23 μg total protein WcfS membrane fraction in the presence of a 20μM NA-BP, all necessary cofactors, and 0.33 mM UDP-GlcNAc (reaction with GlcNAc) or 0.26mM UDP-4-keto sugar (reaction with 4-keto). b) HPLC analysis in 1:1 PrOH/ammounium bicarbonate on C18 of a reaction with 0.1mg PlgF, 0.08mg WcfR and 23 μg total protein WcfS membrane fraction in the presence of a 20μM NA-BP, all necessary cofactors, and UDP-GlcNAc (Reaction) or no sugar (control).

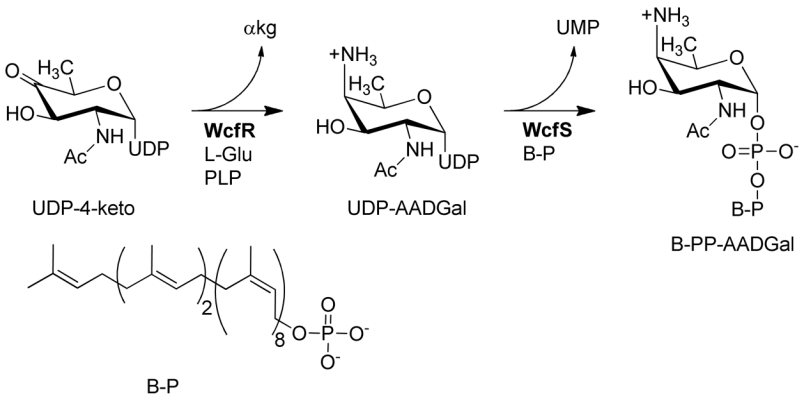

Scheme 1.

Proposed route to the biosynthesis of bactoprenyl diphospho-AADGal. αkg is α-ketoglutarate. B-P is bactoprenyl phosphate

Table 1

1D and 2D NMR of UDP-AADGal

moiety	δ_H (ppm)	J (Hz)	COSY corr	TROESY corr	TROESY integral
uracil					
H5	5.85	8.3	7.84 (H6)		
H6	7.84	8.1		4.24 (H2’/3’), 5.84(H5)	−5.26, −3.76
ribose					
H1′	5.86	4.2	4.26 (H2’)	4.24 (H2’)	−2.08
H2′	4.26				
H3′	4.26		4.17 (H4’)		
H4′	4.17			5.87 (H1’)	−0.58
H5′a	4.08				
H5′b	4.13				
Diphosphate					
Pa	−10.8	20.7			
Pb	−12.7	20.1			
Pyranose					
H1″	5.40	3.5, 7.5	3.97 (H2”)	3.97 (H2”)	−6.02
H2″	3.97		4.11 (H3”)	4.13 (H3”)	−0.84
H3″	4.11		3.48 (H4”)	3.47 (H4”)	−7.12
H4″	3.48		4.43 (H5”)	1.18 (H6”)	−1.46
H5″	4.43		1.19 (H6”)	3.47 (H4”), 4.11 (H3”)	−8.12, −9.16
H6″	1.19	6.9		4.43 (H5”)	−6.83
acetyl	2.06				

COSY and TROESY correlations are provided for each unique peak. T-ROESY integrals are provided as demonstrations of cross-peak magnitude. T-ROESY integrals are negative due to phase dependence of the experiment